# SPRAY-ASSISTED METHOD OF SYNTHESIS OF ANODE MATERIALS FOR LITHIUM-ION BATTERY

**Alina Terechshenko**, BS in Chemical Engineering

**Submitted in fulfilment of the requirements**

**for the degree of Masters of Science**

**in Chemical Engineering**


**School of Engineering**

**Department of Chemical Engineering**

**Nazarbayev University**

53 Kabanbay Batyr Avenue,

Astana, Kazakhstan, 010000

**Supervisor:** Prof. Zhumabay Bakenov,

**Co-supervisor:** Prof. Moulay-Rachid Babaa

**December 2018**

# DECLARATION

I hereby, declare that this manuscript, entitled “Spray-assisted method of synthesis of anode material for lithium-ion battery”, is the result of my own work except for quotations and citations which have been duly acknowledged. I also declare that, to the best of my knowledge and belief, it has not been previously or concurrently submitted, in whole or in part, for any other degree or diploma at Nazarbayev University or any other national or international institution.

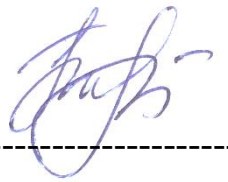

---

Name: Alina Terechshenko

Date: December 13, 2018

# ABSTRACT

The current energy and environment challenges demand an emerging renewable energy sources and green electrical transportation implementation. Both of these require rechargeable batteries to store energy and provide power. However, lithium-ion batteries (LIBs) with graphite-based anode, which is the most used anode material for current LIB technologies, cannot meet the requirements for new generation electric vehicles of different type (hybrid, plug-in or pure) and other applications such as modern communication systems, because they require two to five times more energy density than what LIBs with graphite-based anode can offer. Thus, there is an extreme need for introduction of novel materials for next generation anode for LIBs. The spinel-structured lithium titanium oxide $Li_4Ti_5O_{12}$ (LTO) is one of the most effective active matrices for silicon (Si) to form anode and enhance the advantageous properties of both materials. One of the possibilities to efficiently combine Si and LTO, keeping their advantages and overcoming drawbacks, is to apply nanomixing. Moreover, in order to enhance conductivity of the composite, sucrose and polyethylene glycol (PEG) were added into the material as a carbon source, and their effect on its electrochemical performance was compared. One of the most suitable and promising method of LTO synthesis is the spray pyrolysis technique as there are promising opportunities to establish a continuous preparation process. Another advantage of this method is the opportunity of one-

step operation: the calcination and grinding of the material are not necessary for this type of synthesis. Thus, the powders obtained in the reactor can be directly used as the material for LIBs.

The precursors for LTO were selected lithium nitrate ($LiNO_3$) and titanium tetraisopropoxide (TTIP, $Ti[OCH(CH_3)_2]_4$), which were dissolved in deionized water with the concentrations of 1 M and 0.5 M, respectively. Si nanopowder and carbon sources were also added into the precursors solution. The experimental set-up consisted of droplet generator, quartz-tube reactor and a Teflon filter to collect powder product at the end of the reactor. The droplets were carried into the reactor by nitrogen gas, where the solution underwent a continuous change via the solvent evaporation and formation of a solid precipitate, drying and pyrolysis reaction of the components of the precipitate with expected formation of LTO. The structure and composition of the product were investigated by X-ray diffraction and elemental analysis. The morphology was studied by scanning and transmitting electron microscopies.

The electrochemical performance of the material has been enhanced when the materials were prepared with addition of carbon sources. Both carbon containing samples showed better performance in terms of capacity and cyclability. Furthermore, the efficiency of the sample without carbon additive was dramatically fluctuating within 30 cycles, while the efficiency of the carbon added samples was very stable and delivered 100% of cycling efficiency, which

indicated a low polarization due to the kinetics enhancement by conductive carbon additive. They exhibit stable cycling and efficiency, showing a capacity retention of about 62% after 30 cycles at 0.2 C. In the same conditions the LTO/Si (no carbon) sample retained only 1.2% of its initial capacity.

**Acknowledgments**

I would like to thank my advisor, Professor Zhumabay Bakenov, for introducing me to this research project and guiding towards the completion of the work. Despite busy schedule, he was available whenever I needed and encouraged me for regular progress presentations within the group meetings.

I also want to thank my co-advisor, Professor Moulay-Rachid Babaa, for constant support and help. He always provided me with valuable feedback and guidance.

Finally, I want to express my greatest gratitude to my family and my partner for providing me continuous encouragement and enthusiasm during whole my studies and especially last semester. This achievement would not have been possible without them. Thank you very much.

Alina Terechshenko

**Acknowledgments for research fund support**

This research was supported by the targeted state program No. BR05236524 “Innovative Materials and Systems for Energy Conversion and Storage” from the Ministry of Education and Science of the Republic of Kazakhstan for 2018–2020 (PI Prof. Z. Bakenov) and research project SOE 2017006 “Project Photocatalytic Reduction of CO2 to Hydrocarbon Fuel Using Ternary Metal Oxide on Graphene as 2D Platform” from Nazarbayev University (PI Prof. M.R. Babaa).

# Table of Contents

# List of Tables

# List of Figures

# Chapter 1 – Introduction

## 1.1 Motivation and Objectives

Concerns of energy and ecological crisis are the recognized global issues warranting consideration. These demand the development and rapid implementation of renewable energy sources (solar, wind, hydro, etc.). Due to intermittent and unstable nature of such sources they require reliable and rapid energy storage systems to mitigate the fluctuation and provide smooth integration into the electric grids. Rechargeable batteries are leading a path for such energy storage. Lithium-ion batteries (LIBs), as the best currently available battery technology, have been recognized as a part of pollution-free renewable energy containing grids because they present the most efficient and stable energy storage system for now. LIBs are widely used in many fields and applications because of their small size, slow self-discharging rate, reusability (they can be used over many cycles), high power density and energy. However, LIBs with graphite-based anode, which is the most used anode material for LIBs, are not suitable for modern electric vehicles of different type (hybrid, plug-in or pure) and other modern electronics and communication systems,

because these applications require two-five times more energy density than LIBs with graphite-based anode can offer [1].

The energy density of LIBs can be increased by either changing cathode material to the one with higher potential, or changing anode to the one which has higher capacity. The problem of introducing cathode with high potential is the decomposition of the electrolyte at potentials higher than 4.2 V vs. $Li/Li^+$ [1, 2]. The materials which are mostly used as cathodes in LIBs are the oxides of transitional metals or phosphates such as $LiCoO_2$, $LiMn_2O_4$, $LiCo_{1/3}Mn_{1/3}Ni_{1/3}O_2$, $LiFePO_4$ and others. At the same time, the most popular material for anode is graphite due to its low working potential with lithium, long cycle life and low cost [3]. However, graphite can allow diffusion of only one atom of lithium with six atoms of carbon ($LiC_6$) resulting in a relatively low reversible capacity of 372 mAh $g^{-1}$. Also, the low rate of lithium diffusion into graphite results in low power density of the battery. Thus, there is an extreme need for introduction of novel materials for anode replacement in LIBs. Despite that lithium metal has one the highest capacities of 3860 mAh $g^{-1}$, it is unsafe to use this material as anode in LIBs, because it can cause a short circuit between the electrodes [4].

The electrodes in LIBs are separated by a membrane/separator usually made of polypropylene or polyethylene. The separator is filled (soaked) with electrolyte solution of lithium salts in alkyl carbonates mixture. The purpose of

the separator is to prevent direct contact of the electrodes, i.e. to prevent short circuiting, and allow the flow of lithium ions from cathode to anode and/or vice versa during the processes of charging and/or discharging. During the discharging process electrical energy is produced from chemical energy of reactions. Therefore, the materials utilized in LIBs should maintain good ionic and electrical conductivity, long cycle life (for longer utilization time of the battery), high rate of lithium diffusion into the electrode materials, reversible capacity and low cost.

### 1.2 Literature review on anode materials for anode of LIBs

The list of the suitable anode materials with high capacity for LIBs consists of titanium oxides (175 mAh $g^{-1}$), carbon nanofibers (450 mAh $g^{-1}$), metal sulphides, phosphides and nitrides (500 mAh $g^{-1}$ and higher), tin oxide (780 mAh $g^{-1}$), graphene (960 mAh $g^{-1}$), carbon nanotubes (1100 mAh $g^{-1}$), germanium (1600 mAh $g^{-1}$), and silicon (4200 mAh $g^{-1}$) [5-8]. All of the materials, except metal sulphides, phosphides and nitrides, have the common feature which gives the new perspectives to the development of anode materials for LIBs – nanostructure. The abovementioned exclusions cannot be used as effective anode, because of high volume expansion, which leads to the deformation of the battery, low coulombic efficiency, capacity fading and low electron transport [9]. The main advantages of using nanostructure of potential

anode materials are high volume-to-surface ratio, which leads to the increase of active sites on the anode surface and more lithium ions can be stored, meaning increase in specific capacity, perspectives in the investigation of the electrochemical reactions in bulk solutions, increase of power capability due to more effective lithium diffusion, higher rates of electrons transfer [10, 11]. Further, a brief description of the most suitable potential anode materials will be presented.

### 1.2.1 Carbon-based materials

Carbon nanotubes (CNTs) are presented by two types: single-walled CNTs (SWCNTs) and multi-walled CNTs (MWCNTs) distinguished by the number of graphene layers. They are widely used in combination with other active materials, because they improve the overall performance of the material used due to their transcendent electronic conductivity, mechanical and thermal stability, adsorption and transport properties [12]. The theoretical capacity of SWCNTs in $LiC_2$ was shown to be 1116 mAh $g^{-1}$, and considered as the highest theoretical capacity among all the carbon-based active anode materials [13]. In 2010, DiLeo et al. obtained the capacity of 1050 mAh $g^{-1}$ of SWCNTs which were synthetized by laser vaporization [14]. However, the researches have not yet come up to the methodology which could allow to obtain high and stable coulombic efficiency and high lithium storage capacity. Thus, the utilization of

CNTs as active anode material is promising but still challenging. In addition, the production of LIBs with CNTs is not commercially beneficial because of high cost of the nanotubes.

Graphene can be described as a network of sp2 carbons bonded into 2-dimensional sheet with single-atom thickness. Graphene obeys excellent electrical conductivity, mechanical strength, high surface area and high charge mobility [6]. Several graphene sheets can adsorb higher amount of lithium ions in comparison with graphite leading to the higher electrical capacity which is estimated to be 780 and 1116 mAh $g^{-1}$ [6]. The values differ because of the ways of lithium ions adsorption reported: in first case the ions were absorbed by the inner and outer faces of graphene sheets (1 to 6 stoichiometric ratio), meanwhile the second one reported lithium ions to be trapped in a covalent bonding in the benzene rings (1 to 2 stoichiometric ratio). Recently it was suggested to use the combinations of graphene with metals, metal oxides and phosphides. For instance, the combination of graphene oxide sheets with silicon composite showed high capacity of 1600 mAh $g^{-1}$, high coulombic efficiency during 100 life cycles [15].

### 1.2.2 Titanium-based materials

Titanium oxides have several remarkable features which are maximum safety, low cost, low toxicity, volume stability (1-3% change) and long life duration

[16, 17]. On the other hand, titanium oxides have low theoretical capacity (175-350 mAh $g^{-1}$) and low electronic conductivity [9]. Therefore, they are mainly used as additive to the other active materials to improve capacity, cycling and rate capability [18]. The most efficient combination of titanium dioxide is the spinel $Li_4Ti_5O_{12}$ (LTO), because of superior Li-ion reversibility at relatively high operating potential of 1.55 V vs. $Li/Li^+$. One of the advantages of this compound is the stability of structure during the insertion of Li-ions [16, 19]. Because of that, the solid electrolyte interface (SEI) does not form and dendrites formation, which is of the most concern in carbon-containing anodes, is avoided. However, despite of the safety conditions which brings the usage of LTO and its suitability as anode in LIBs, there are some drawbacks of this compound. It has very low theoretical capacity (175 mAh $g^{-1}$) and low electronic conductivity (10-13 S $cm^{-1}$) leading to the reduction of the diffusion rate of Li-ions into the structure and charge-discharge rate [20]. Thus, there is a need for treatment techniques to overcome these problems, which will be discussed further.

One of the methods is to bring the compound to nanoscale. Prakash et al (2010) reported the way of synthesis of nano-crystalline LTO with size range of 20-50 nm by solution combustion method [21]. The result of his experiment is the achievement of 170 mAh $g^{-1}$ of discharge capacity at 0.5 C current rate.

### 1.2.3 Alloy and Oxide anodes

Other materials which can be used as the advanced anodes in LIBs are the materials whose mechanism of reaction with lithium metal is similar to the one of alloys and de-alloys. These materials are mainly represented by silicon, germanium and tin oxide. The theoretical capacity of these components is much higher than of above described materials, ranging from 780 mAh $g^{-1}$ (SnO) to 4200 mAh $g^{-1}$ (Si) [22]. However, the main drawback of these materials is the short durability (number of cycles) and high deformation due to the volume increase. There are certain techniques to overcome these difficulties, which are bringing the materials to nanoscale, as previously described, and formation of a matrix of active and inactive materials [23]. The last one is the most perspective method and will be discussed later.

Silicon is the component, which in chemical compound with lithium ($Li_{22}Si_5$) can reach the highest possible capacity of 4200 mAh $g^{-1}$ among the materials which have been discussed [24]. It has low discharge potential of 0.4 V which is comparable with graphite. In addition, there is sufficient amount of silicon on the earth, which makes it inexpensive and environmentally friendly material. However, the changes in volume almost by 360-400% during charging and discharging damages the structure of the battery and causes short cycling life, irreversibility of lithium extraction and capacity damping [25]. Consequently, to overcome the above presented problems many efforts have been made: for

instance, Park et al. achieved high specific capacity of 865 mAh $g^{-1}$ at 0.5 C, significant improvement of volume change (increase by 42% after 200 cycles), and superior cycle and rate stabilities by producing Si nano-sheets using natural clays and molten salt-induced exfoliation [26]. Also, the transcendent results were obtained by Chan et al when the direct growth of Si nano-wires on the metallic collectors were performed [27]. Due to the direct electronic contact of Si nano-wires with current collector, all the nano-wires took place in the alloy process, good charge transport mechanism become possible, and the volume increase was easily fitted because of small diameter of Si nano-wires. The results of this experiment were 3500 mAh $g^{-1}$ of the specific capacity at 0.2C rate (for 20 cycles) and 2100 mAh $g^{-1}$ at 1C rate. However, despite the superior effectiveness of the methods described above and other methods developed by the researches to improve suitability of the Si in anode of LIBs, these techniques are not commercially reasonable making them not applicable for the industrial scale. Consequently, alternative methods for materials fabrication are developed such as formation of matrices of active and inactive materials mentioned above.

There are many techniques to fabricate these matrices such as spray-drying methods (e.g. spray pyrolysis), dry ball milling, wet ball milling, hydrothermal and solvothermal methods. For instance, Chan et al. conducted the experiment, where they grew the carbon coated Si nano-wires in liquid solution by mixing of nano-wires with conductive compounds such as multi-walled CNTs and

amorphous carbon [28]. The results gave the reversible capacity of 1500 mAh $g^{-1}$ at 0.2 C rate and 200 cycles. Song et al. formed tubular silicon nanostructures using the techniques of chemical vapor deposition (CVD) [29]. The charging-discharging capacity achieved the value of 3360 mAh $g^{-1}$, and stable capacity of 2600 mAh $g^{-1}$ at 0.2C rate.

Germanium is the active anode material with theoretical capacity of 1600 mAh $g^{-1}$ in similar to Si chemical compound of $Li_{22}Ge_5$. The advantages of Ge are much higher electrical conductivity and faster diffusion rate of lithium into Ge structure in comparison with Si, and higher anode capacity compared to graphite. Thus, Ge has higher rate capability and higher charge transport in comparison with silicon and graphite. However, Ge is much more expensive than Si and has the same drawback – significant change of volume during lithiation-delithiation (up to 300% increase) [30]. The best techniques to overcome this involve using of conductive matrices synthetized by solid-state pyrolysis. For instance, Ge nanoparticles encysted in carbon nanospheres (the diameters are 5-20 nm and 50-70 nm) showed high lithium storage and high rate capability, because nanospheres performed as a buffer and conductive material during the lithiation and delithiation processes and prevented the direct contact of the material and electrolyte solution which leaded to non-formation of SEI.

*Tin oxide* is attractive as potential anode in LIBs because of its high theoretical capacity and low working potential (782 mAh $g^{-1}$ and 0.6 V,

respectively). In addition, $SnO_2$ has low cost, it is abundant and eco-friendly material. However, this material has the same drawback as other metal oxides – dramatic volume change (more than 200%) and consequently low cycling performance. Because of that, the porous structures of tin oxide are preferred as they possess high capacity and high rates of lithium ions diffusion [31]. Yin et al. after the experiments with mesoporous spheres of $SnO_2$ (100-300 nm diameter) stated that porosity in the nanostructure of the material can compensate the volume increase during lithiation process [31]. Significant attention is paid to the development of carbon based composites as coated tin oxide, or tin oxide in combination with carbon nanoparticles, etc. The results are the better storage capacity, cycling life and coulombic efficiency (about 550 mAh $g^{-1}$ and 100 cycles). Recently, many morphological structures of tin oxide were investigated: nanotubes, nanorods, nanosheets, nanoboxes, nanowires [32, 33]. Also, the experiments were conducted to obtain the optimum length of nanotubes and it was reported by Ye et al that shorter nanotubes show better capacity and cycling life (470 mAh $g^{-1}$ and 30 cycles) [32].

The summary based on the data described above can be viewed in Table 1.1. As it can be seen each of the potential advanced anode material has its own advantages and drawbacks, which can be effectively used in the regard of the application purpose.

***Table 1.1: Advanced anode materials for LIBs***

| Potential anode material | Theoretical capacity (mAh $g^{-1}$) | Advantages | Drawbacks |
|---|---|---|---|
| *Carbon-based materials [6, 12, 13, 15]* | | | |
| Carbon nanotubes | 1116 | Safe<br>Low cost<br>High working potential | Low reversible capacity<br>Instability at high potential<br>Low efficiency |
| Graphene | 780-1116 | | |
| *Titanium-based materials [9, 16-20]* | | | |
| Spinel LTO | 175 | Safe<br>High cycling life<br>Low cost | Low capacity<br>Low energy density |
| *Alloys and Oxides [22-25, 30-33]* | | | |
| Silicon | 4200 | Safe<br>High specific capacity<br>High energy density | Low reversible capacity<br>Drastic volume expansion<br>Short cycling life |
| Germanium | 1600 | | |
| Tin oxide | 780 | | |

### 1.2.4 Materials selection

As a conclusion, it can be stated that silicon is one of the best materials for anode in LIBs, as it is of low cost, abundant and environmentally friendly material with huge theoretical capacity of 4200 mAh $g^{-1}$ for $Li_{22}Si_5$. It obeys low operation potential about 0.5 V *vs.* $Li^+/Li$, which results in a high energy density in full cells operated on Si anodes [34]. In addition, the lithiation/delithiation potential of Si is higher than that of Li, resulting in the electrode with a safer applicability. However, it is impossible to use it solely as anode in LIBs because of the severe volume expansion during the lithiation process. Therefore, there is a need for other material or materials to fabricate abovementioned matrix of active and inactive material to overcome this problem. Thus, spinel-structured

lithium titanium oxide $Li_4Ti_5O_{12}$ is one of the most effective active matrices for Si to form anode and prevent the dramatic volume expansion. As it was described LTO has high stability of the structure and about 0.2% of possible volume changes during the lithium ion diffusion. Also, it has good characteristics to be considered as potential anode, in particular flat potential of 1.55 V vs Li+/Li, which prevents the formation of SEI and Li dendrites. However, at low potentials (about 0 V) electrolyte can decompose and SEI can appear leading to the increase of the risk of high irreversibility and the damage of the whole battery [35]. In addition, LTO is distinguished by the low diffusion rate of lithium ions and low electrical conductivity ($10^{-11}$ $cm^2$ $s^{-1}$ and $10^{-13}$ S $cm^{-1}$ respectively).

One of the possibilities to efficiently combine Si and LTO keeping their own advantages and overcoming drawbacks is to apply nanomixing. It can be assumed that after mixing of Si and LTO, the final product will have the main features of both materials: high capacity and stability of cycling life omitting the volume expansion of Si. Recently, Chen et al investigated the anode composite of LTO/Si [36]. As it was already mentioned, both LTO and Si have low electronic conductivity, therefore, the conducting medium, in particular carbon based material, is required.

The carbon sources are often added into material in order to enhance the electrochemical properties. Sucrose, glucose, starch and some acids can be

effectively used as carbon sources [37]. Therefore, it was decided to add sucrose and polyethylene glycol (PEG) separately as carbon sources into the material, and to compare their effect on the electrochemical performance. Overall, three types of the battery are obtained and compared: LTO/Si, LTO/Si/Sucrose, LTO/Si/PEG.

### 1.3 Literature review on synthesis techniques

Hong et al. reported solution combustion and solution precipitation methods of synthesis of LTO and $Co_3O_4$ [38]. It was stated that the obtained structure of the composite appeared to be a cubic spinel structure. Attached particles of cobalt oxide on the surface and in the pores of LTO prevented the volume expansion of cobalt oxide material. As a result, the capacity of LTO was increased to 300 mAh $g^{-1}$. The method of solution combustion was used to develop LTO component. For this purpose, titanium (IV) isopropoxide [$Ti\{OCH(CH_3)_2\}_4$] (TTIP) was added drop-by-drop to the distilled water at 10 $^oC$. After white precipitation of the compound appeared, the mixture was actively stirred until it became colorless. The next step is the dissolution of lithium nitrate and addition of fuel – glycine. The mixture was left at continuous stirring for 5 h which resulted in a viscous fluid similar to gel. After that, the alumina crucible was heated to 500 $^oC$ and the precursor was dropped to it. Then it was heated for 12 h in muffle furnace. The composition of LTO and cobalt

oxide was done by precipitation of cobalt-ions: $Co(NO_3)_6 \cdot H_2O$ was dropped to preliminary dispersed LTO in distilled water in a mass ratio of 20:40. As a finishing step, $NH_4OH$ was added to the mixture and stirred for 2-4 h. The obtained precipitate was filtered and washed 3 times and then dried in vacuum furnace at 80 $^oC$ for 12-13 h. The resulting powder was further calcined at 450 $^oC$ for an hour in air.

Prakash et al. described a similar technique of synthesis of nanocrystalline LTO by solution combustion [39]. As a result, the capacity of LTO reached its theoretical value and life of the anode was computed as 100 cycles. The reactants were titanyl nitrate $[Ti(NO_3)_2]$ and lithium nitrate $LiNO_3$; glycine was again used as a fuel. The components were mixed at the following ratio: 0.0362 mol of titanyl nitrate, 0.0289 mol of lithium nitrate and 0.0562 mol of glycine. The mixture was transferred to the alumina crucible and heated in muffle furnace at 800 $^oC$. The reaction occurs in several seconds. After the mixture was cooled, the obtained solids were crushed into powder by mortar and pestle.

Jiang et al. obtained nanocrystalline LTO by lithiation of anatase nanocrystals [40]. The obtained LTO showed higher capacity and stability. The experimental procedure starts with dissolution of 0.4 g of anatase powder in 100 mL of 2.5 M lithium hydroxide in a Teflon flask, which was subsequently put into water bath and kept stirred for 10 h at 60 $^oC$. After that, the sample was cooled and washed

with distilled water and ethanol several times, and put into vacuum furnace at 70 $^{o}$C for complete drying. Finally, the product was annealed at 600-700 $^{o}$C for 3-5 h in air.

Huang and Jiang reported about macroemulsion method for hollow spherical LTO synthesis [41]. The results are the durability of over 500 cycles with the capacity of 140 mAh $g^{-1}$. Firstly, 2 g of P123 (poly(ethylene oxide)-block-poly(propylene oxide)-block-poly(ethylene oxide) triblock copolymer, shortly $(EO)_{20}(PO)_{20}(EO)_{20}$)) and 1.51 g of $Li(CH_3COO)\cdot 2H_2O$ were dissolved in 20 mL of ethanol. Then, 100 mL of n-heptane with 5.47 g of $Ti(OC_4H_9)$ was added to the above mixture and stirred at room temperature. During stirring, 5 mL of distilled water was added to the solution. The mixture then appears as dense and white colloid suspension. The mixture is kept being stirred for 3 h, and then is dried at 65 $^{o}$C for total riddance of the liquid. The precursor was calcined at $O_2$ atmosphere from room temperature to 350 $^{o}$C with ramp of 2 $^{o}$C $min^{-1}$, then the temperature was increased to 750 $^{o}$C with ramp of 5 $^{o}$C $min^{-1}$ and left for 10 h.

Cheng et al. increased the capacity of LTO by thermal vapor decomposition of LTO. As a result, a 5 nm thick carbon-layer was applied on the surface of LTO [42]. The raw materials, titanium (IV) oxide and lithium carbonate, were mixed at ratio of 5:2 respectively, and heated at 800 $^{o}$C for 24 h. Then, the raw LTO was transferred to reaction tube for reaction with toluene vapor by nitrogen gas with volumetric flowrate of 1 L $min^{-1}$ at 700-900 $^{o}$C for 2 h. The electrode

then was prepared by mixing 95 wt% of active material (LTO), 5 wt% of carbon black, and 5 wt% of polymer (poly(tetrafluoroethylene)).

Kavan and Gratzel reported about sol-gel route synthesis of monocrystalline LTO which resulted into transcendent activity during lithiation process [43]. 1.4 g of lithium was dissolved in 110 mL of ethanol at argon atmosphere. This solution was mixed with 71 g of titanium (IV) isopropoxide (it can be substituted by 85 g of titanium (IV) n-butoxide). 50 mL of obtained solution was hydrolyzed in 300 mL of water. The resulted slurry was transferred on a rotary evaporator, with operation conditions of 20 mbar and 40 $^{o}$C. Polyethylene glycol was added at the ratio of 1:2 to LTO solution, and the obtained mixture was stirred for 12 h. The resulting liquid was annealed at 500 $^{o}$C for 30 min.

Jin et al. proposed method of the urea-forced hydrolysis and precipitation below 100 $^{o}$C [44]. Titanium (IV) oxide nanoparticles were prepared from 0.015M titanium trichloride ($TiCl_3$) and 3.03M urea ($(NH_2)_2CO$) dissolved in deionized (DI) water. Then, the solution was heated to 100 $^{o}$C and stirred for 4 h. The obtained precipitate was washed with DI water and then with ethanol and put into vacuum oven for drying for 6 h. Preparation of LTO was performed by two methods. The first one starts with dispersion of titanium oxide nanoparticles in DI water by sonication for 2 h. After that, lithium hydroxide was dissolved in the solution. Then the obtained mixture was heated to 100 $^{o}$C for water evaporation and calcined in air. The second method includes high-

energy ball milling of the same components at the same ratio as described above, excluding the dispersion in water. The results are prolonged cycle performance of 500 cycles and enhanced capacity after the 500$^{th}$ cycle (130 mAh g$^{-1}$).

Birozzi et al. used a large scale flame spray pyrolysis (FSP) to synthetize a nanoscale LTO [45]. The result of this experiment, was a stabilized composite with up to 1000 cycling life. The authors investigated different ratios of materials to obtain the optimum. The experimental procedure includes dissolution of titanium (IV) 2-ethylhexanoate and lithium acetate dehydrate (also lithium hydroxide may be effectively used) in organic solvent. The solution was fed to the nozzle of FSP. The operation conditions are the following: volumetric flowrate of feed of 0.03 L min$^{-1}$, volumetric flowrate of oxygen dispersion of 30 L min$^{-1}$, and pressure drop of 1 bar across the nozzle. The volumetric flowrate of shell gas was set as 40 L min$^{-1}$ during the whole operation. The flame was supported by 3.2 L min$^{-1}$ of oxygen and 1.5 L min$^{-1}$ of methane. The obtained product was collected by Baghouse filter system.

Kim et al. also used FSP technique for LTO production [46]. The precursors were TTIP and lithium nitrate solutions with concentration of 0.5 M dissolved in the mixture of ethanol and distilled water (3:7 respectively); flame was provided by mixture of propane and oxygen gases. The ultrasonic nebulizer was used as a droplet generator; the droplets were delivered into the high-temperature

diffusion flame by oxygen as carrier gas. Prepared powders (collected into bag filter) were post-treated in the furnace at 600-800 $^{o}$C for 3 h under air.

Wu et al. used spray-drying method for LTO synthesis [47]. The titanium precursor was TTIP dissolved in DI water; in order to eliminate the obtained precipitation $H_2O_2$ was added into the solution and mixed with 12.5% ammonia solution (pH around 10). The lithium precursor was produced by dissolving 96wt% of $LiOH \cdot H_2O$ in DI water. The above solutions were again mixed in DI water at specific proportions. The solution was processed in spray drier machine (SD-2500) delivered by peristaltic pump at rate 300 mL $h^{-1}$. The process temperature and pressure were set 200 $^{o}$C and 0.2MPa. The produced powders were calcined under air at different temperatures from 650 to 800 $^{o}$C for 16 h.

Ju et al. used the similar technique for LTO production [48]. The authors used TTIP and $LiNO_3$ both dissolved in distilled water as the precursors with various concentrations. The ultrasonic nebulizer was used to generate droplets, which are delivered into quartz reactor by carrier gas. The powders were deposited in the reactor; the reactor temperature was varied from 600 to 1000 $^{o}$C, the carrier gas flowrate was also varied from 10 to 40 L $min^{-1}$.

As a result, the most suitable and promising method of LTO synthesis could be the gas-state technique, spray pyrolysis method, as it can be further developed and investigated and there is promising opportunity to establish a continuous preparation process. One more advantage of this method is the

opportunity of one-step operation: the calcination and grinding of the material are not necessary for this type of synthesis. Thus, the powders obtained in the reactor can be directly used as the material for LIBs. Also, according to Wu et al. and Ju et al. it is possible to add Si nanopowder into the precursor solution and process the mixture as it was described [47-48]. The resulted powders contained nanosized particles with spherical shape. Moreover, the above methods are the most suitable to be used with the University facilities.

Therefore, it was decided to proceed with the preparation of LTO material using the above mentioned modified method. The modifications are required to the described process, as Si, sucrose and PEG will also be added into the precursor solution, which will be discussed in the further chapter.

# Chapter 2 – Experimental procedures

## 2.1 Materials preparation

As it was shown from the literature review, the starting materials were selected as lithium nitrate and titanium tetraisopropoxide illustrated in Fig. 1 below. The precursor solutions were prepared by dissolving lithium nitrate ($LiNO_3$, 98%, Sigma Aldrich) and titanium tetraisopropoxide (TTIP, $Ti[OCH(CH_3)_2]_4$, 97%, Sigma Aldrich) in distilled water. The concentration of the precursor solutions was 1 M for lithium precursor and 0.5 M for titanium precursor as it appeared in the experiments that titanium precursor gives excess of the metal for equimolar concentrations, which leads to the creation of rutile $TiO_2$ in significant amounts (up to 30% for 0.5 M of Ti and Li). Also, preparation of titanium solution required addition of some drops of hydrochloric acid (37%, Sigma Aldrich); then, it is left at stirrer over night for complete dissolution of TTIP. Then, the solution was mixed with Si nanopowder (30-50 nm, Guangzhou Jiechuang Trading Co.). 0.6 gram of Si nanopowder was added to the 100 mL of precursors solution (per 50 mL for lithium and titanium).

***Figure 2.1: The chemical structures of a) Lithium Nitrate;***

***b) Titanium Tetraisopropoxide***

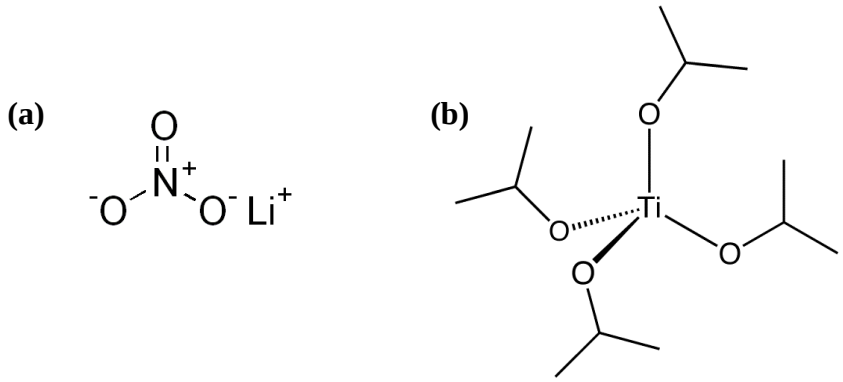


Two carbon sources were investigated during the project: sucrose (Skat Reactiv) and polyethylene glycol (PEG, Sigma Aldrich). The objective was to study the effect of non-polymeric and polymeric carbon source for the electrode performance and to compare it with performance of the material without any carbon additve. For these experiments, the sucrose and PEG were dissolved in above described solution in the amount of 16 g and 3 g respectively, taking into account their solubility in water.

## 2.2 Apparatus set-up

The spray-drying system, illustrated in Fig. 2 below, consists of the droplet generator (nebulizer, OMRON), quartz-tube furnace and filter introduced at the exit of the reactor. The dimensions of tubular reactor are 120 cm in length and 6 cm in diameter. The heating belt was introduced at the exiting part of tube, as the tube was too long for the furnace. The nebulizer was used to generate

aerosol flow which was directed into the high-temperature quartz-tube reactor by the carrier gas ($N_2$). The Teflon filter is located at the exit of the tube to catch the flowing particles. The temperature of the tube furnace was set 800 ºC and the temperature of the heating belt was 315 ºC (which was the maximum technically set).

***Figure 2.2: The schematics of the experimental set-up***

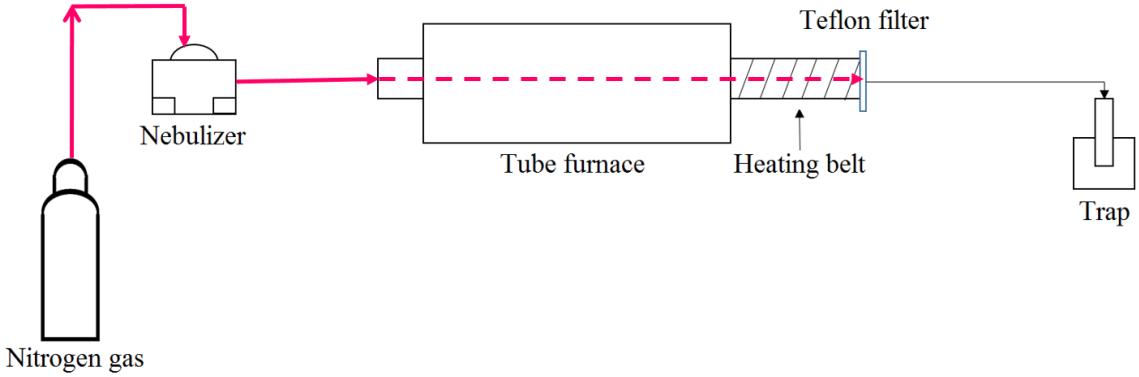


There were some modifications of the set-up during the process.

Firstly, at the early stages of the experiments, the precursor solution was fed into the nebulizer by peristaltic pump at the rate 1 rpm. However, as it was concluded (based on the literature review) that the optimum gas flowrate was 4 L $min^{-1}$, the speed of the precursors solution consumption for aerosol generation and, consequently, the precursors solution supply by the pump were too low and the aerosol generated was blown back to the beaker with the precursor solution through the pipe by the gas flow. Thus, the peristaltic pump

was removed and the solution was supplied manually through the injections with medical syringe in the pipe in order to avoid air intake in the reactor.

Secondly, for the experiment without carbon source, the ultrasonic nebulizer was used. For the experiments with carbon sources the concentration of metal precursors was lowered twice: 0.5 M for $Li^{+}$ and 0.25 M for $Ti^{2+}$ in order to decrease the viscosity of the precursors solution. However, even with those concentration ultrasonic nebulizer could not generate aerosols as the sticky solution deposited on the walls of the cup of the nebulizer (Fig. 2.3). Therefore, the compressor nebulizer was utilized as it is more suitable for "thicker" solutions. The main drawback of this type of nebulizer is that it uses outside air in order to generate the droplets, even though the gas was introduced in it.

***Figure 2.3: The two types of nebulizers used in the project: a) ultrasonic; b) compressor***

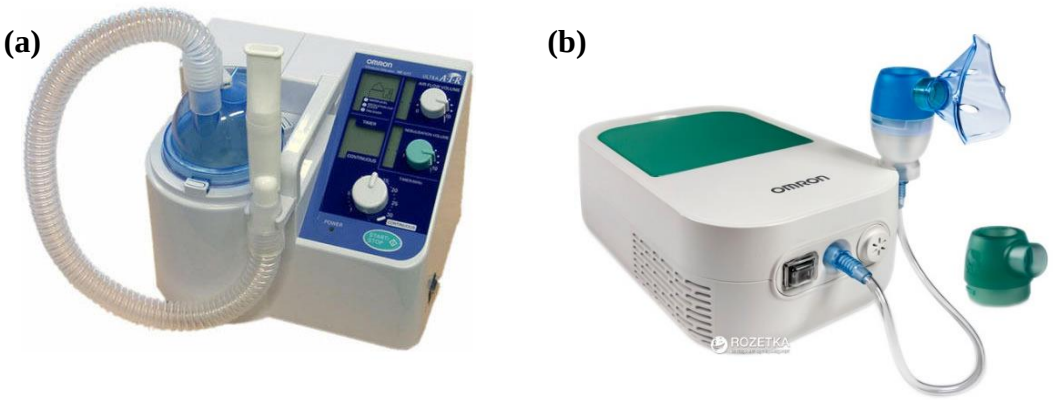


The ultrasonic nebulizer was used at maximum air-flow volume and nebulization volume. The compressor nebulizer did not have those options. The

sealing of the nebulizers was provided by the PTFE sealing tape and silicon paste.

### 2.3 Cell configuration

In order to perform the electrical testing, the assembling of the batteries should be done. The CR2032 coin cells were assembled in a glovebox (MasterLab, MBraun) with lithium foil as both counter and reference electrode. Firstly, the electrode was prepared from the material produced by the experiment described above. For this purpose, the slurry was made from active material, acetylene black (AB, Arkema) and carboxylmethyl cellulose (CMC, MTI). 10 g of CMC was preliminary dissolved in 600 mL of DI water for better mixing with the powders. The above components were mixed in an agate mortar for 20-30 min till a homogeneous mixture was obtained with the following proportions of the components: 80 wt% of active materials, 15 wt% of AB and 0.5-0.6 mL of CMC solution. When the slurry was uniform color and did not contain any solids and bubbles, it was applied on a copper foil using doctor blade technique with a thickness of 5 μm. This followed by drying at 60 °C for 2 h in a vacuum oven and roll-pressing. After this, the electrodes were cut into circles with diameter of 15 mm.

The parts of coin cells were washed in ethanol in an ultrasonic bath for 30 min, and then dried in a vacuum oven for 4 h. Then, the parts of coin cells and electrodes were preliminary welded in the following order: positive cap → spring→ spacer→ electrode (by two ends). The cells were assembled in a glove box under argon atmosphere (Ar, 99.9999% purity). Polypropylene microporous Celgard 2300 film was used as a separator. 1 M lithium hexafluorophosphate ($LiPF_6$) in ethylene carbonate (EC), ethyl-methyl carbonate (EMC) and dimethyl carbonate (DMC) (1:1:1 by volume) (Targray) was utilized as electrolyte. The assembling was done in the following order: welded parts→ 2-3 drops of electrolyte→ separator→ 2 drops of electrolyte → lithium foil → negative cap. Then, the cell was pressed by the crimper to seal it hermetically.

### 2.4 Structural characterization

The prepared samples were characterized by X-ray diffraction (XRD, Rigaku SmartLab) at Cu-Kα radiation (λ = 0.15406 nm) within 2θ range of 10-80°. The interpretation of the XRD data was performed using Match! 2 software which uses COD-Inorg REV173445 2016.01.04 database. Thermal gravimetric analysis (TGA, SDT-Q600, TA Instruments) was also done for the precursor solutions of Li and Ti at molar proportion as 4:5 for Li and Ti respectively. The analysis was performed in nitrogen in a temperature range of 0-1000 °C and a heating rate of 20 °C $min^{-1}$. The morphology and structure of the samples were

studied using scanning electron microscopy (SEM, Zeiss CrossBeam 540) and transmitting electron microscopy (TEM, Jeol JEM-1400Plus). The presence of carbon sources in the sample was checked by XRD, CHNS (Abacus, GMBH) analysis and energy-dispersive X-ray spectroscopy (EDS, Zeiss CrossBeam 540).

## 2.5 Electrochemical characterization

The electrochemical characterization was performed on multichannel battery tester (BT-2000 Arbin Instruments Inc.) at room temperature within a potential range of 0.01 - 3V (vs. Li+/Li). The appropriate current and capacity were calculated as following:

$$I = q \times m \times Crate, \tag{2.1}$$

where $I$ is current, mA;

$q$ is the theoretical capacity, mAh $g^{-1}$;

$m$ is the mass of the active material, g;

$Crate$ is the current rate, $h^{-1}$.

$$q = \sum q_i \times x_i, \tag{2.2}$$

where $q_i$ is the theoretical capacity of the component i;

$x_i$ is the mass fraction of the component i in total mass of the material.

The theoretical capacities of Si and LTO were taken as 3700 [49] and 175 mAh $g^{-1}$, respectively. The mass of active material was calculated based on the weight of the active parts such as LTO, Si, AB and carbon sources. In details, the mass of slurry on the electrode was obtained by weighting the electrode and subtracting the mass of copper foil of the same diameter from that mass. The mass fractions of the LTO, Si and carbon components were defined based on XRD patterns. Then, the mass fractions of LTO, Si, carbon sources and AB were subtracted from the mass of slurry, giving the active mass which is used in equation (2.1).

# Chapter 3 – Results and Discussion

## 3.1 Results of structural characterization

As it was stated before, the goal of the project is to prepare the novel anode material for Li-ion battery by spray-assisted method. It was decided to synthetize LTO because of its ease in operation and promising electrochemical properties. The characteristics of this material should be potentially improved by addition of silicon and carbon source by nanomixing. In order to optimize and improve the process, all the components were preliminary mixed. Hence, three types of powders were obtained based on the content: LTO/Si, LTO/Si/Sucrose, LTO/Si/PEG. TGA-DTA analysis was performed for Li and Ti precursors solution mixed at molar ratio 4:5 respectively. The results are presented below in Fig.3.1.

***Figure 3.1: The TGA results of Li and Ti precursors***

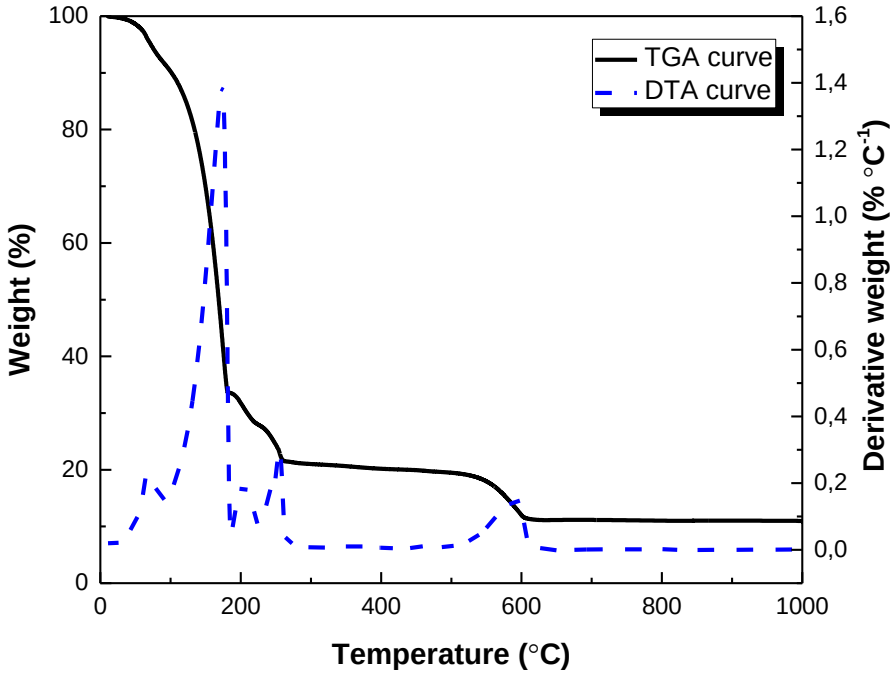


The thermogram can be divided into the three regions. In the first region, the weight loss between temperature range of 60–100 ºC could be related to water removal from the sample. The second region between 180 ºC and 250 ºC comprises of two weight loss (the second and third DTA peaks in Fig. 3.1) which could be associated probably with the loss of $CO_2$ and $NH_2$. The final stage is the decomposition of the remaining residuals into LiO and $TiO_2$ occurring in the temperature region of 523–590 ºC. The plateau after this region shows the stability of the sample after 600 $^0$C.

The XRD analysis was done after each experiment. The results of XRD analysis of the successful experiments are presented in Fig. 3.2.

***Figure 3.2: XRD patterns of: a)LTO/Si, b)LTO/Si/Sucrose, c)LTO/Si/PEG***

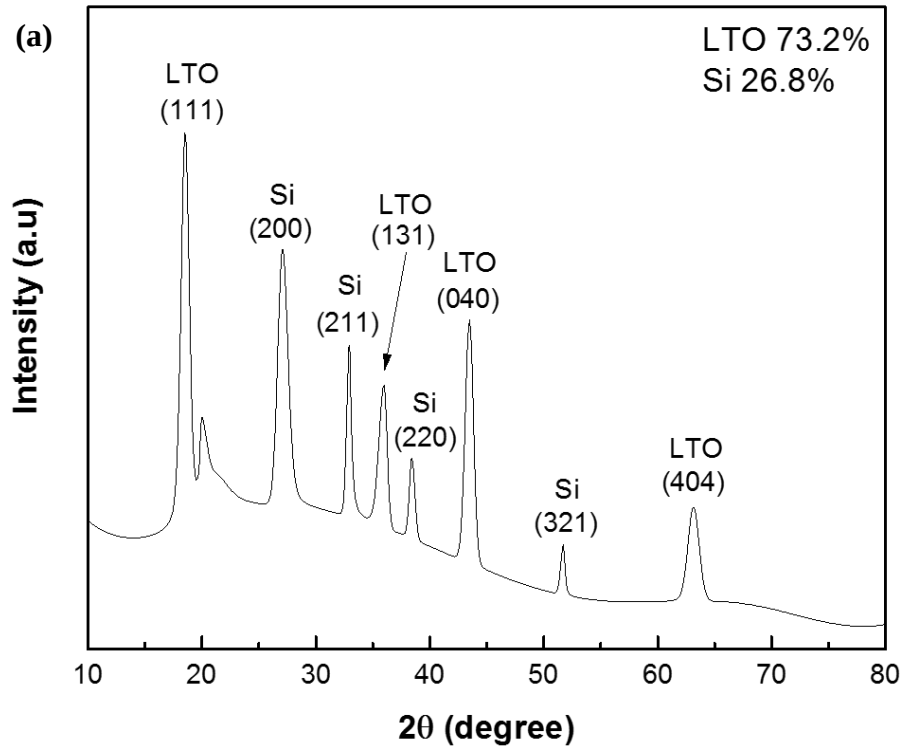


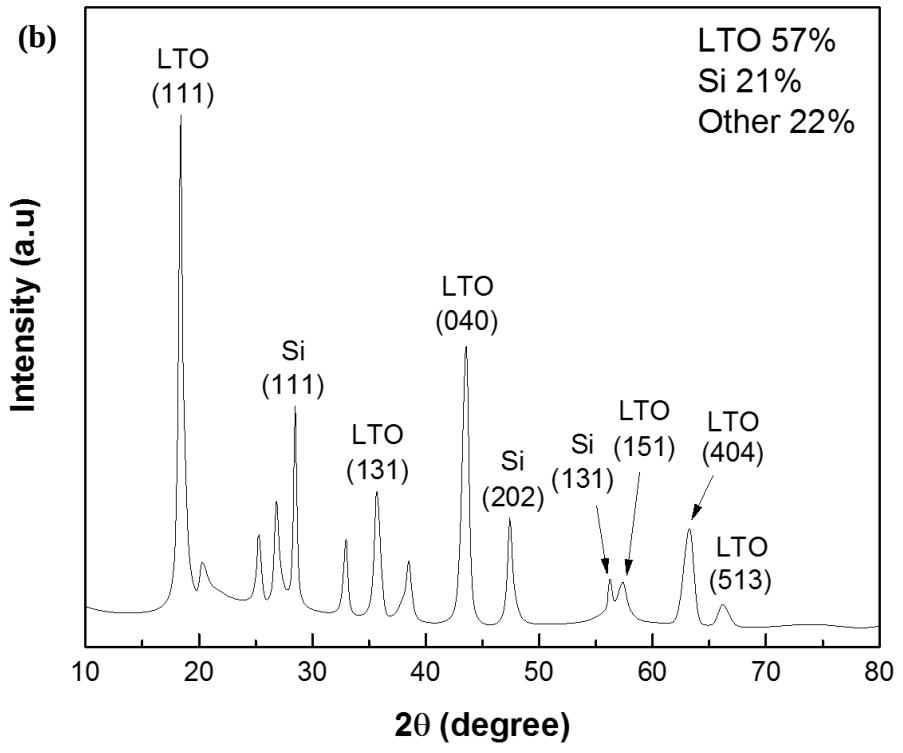

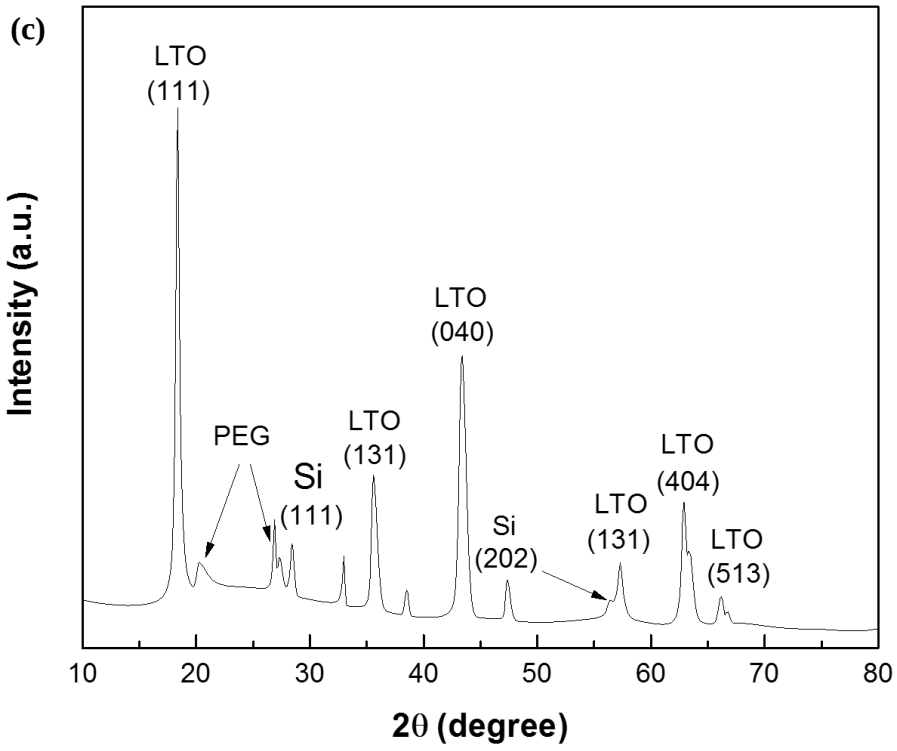


Because of disability of Match! 2 software to recognize polymeric compounds, the peaks of PEG were defined manually based on Barron et al., which corresponded this feature to 19.23° and 27.32° [50]. Thus, two peaks could be possibly assigned to PEG in the sample. Nevertheless, as it can be seen from the patterns above, the presence of carbon sources was not revealed by XRD analysis.

The calcination of both samples was performed at the temperature of 800 °C for 4 h in nitrogen in order to ensure the carbonization of carbon sources added. However, after XRD of the resulting powder, it appeared that most of LTO was converted into rutile $TiO_2$, and peaks of Si also disappeared. The possible reason for this could be a low purity of the nitrogen gas (as the technical grade gas was

used). Thus, it was decided to use as-prepared powders without calcination. In order to know the carbon content, CHNS analysis was performed for two samples. The results are presented in the Table 3.1.

***Table 3.1: CHNS results***

| | **LTO/Si/Sucrose** | **LTO/Si/PEG** |
|---|---|---|
| N Area | 1 144 | 1087 |
| C Area | 178 | 252 |
| H Area | 665 | 1247 |
| S Area | 54 | 51 |
| N [%] | 1.69 | 1.64 |
| C [%] | 0.36 | 0.52 |
| H [%] | 0.461 | 0.871 |
| S [%] | 0.158 | 0.151 |
| C/N ratio | 0.2153 | 0.32 |
| C/H ratio | 0.7872 | 0.6025 |

As it can be seen from the Table 3.1, the amount of carbon is very low in both samples. The possible reason could be the fact, that most of carbon burned at the inlet of the tube and the majority of it was converted to carbon monoxide and carbon dioxide because of the air intake by the compressor nebulizer, which was discussed earlier. The interesting results were obtained by SEM and TEM images presented in Fig. 3.3.

***Figure 3.3: SEM images of: a) LTO, b)LTO/Si, c)LTO/Si/Sucrose, d)LTO/Si/PEG***

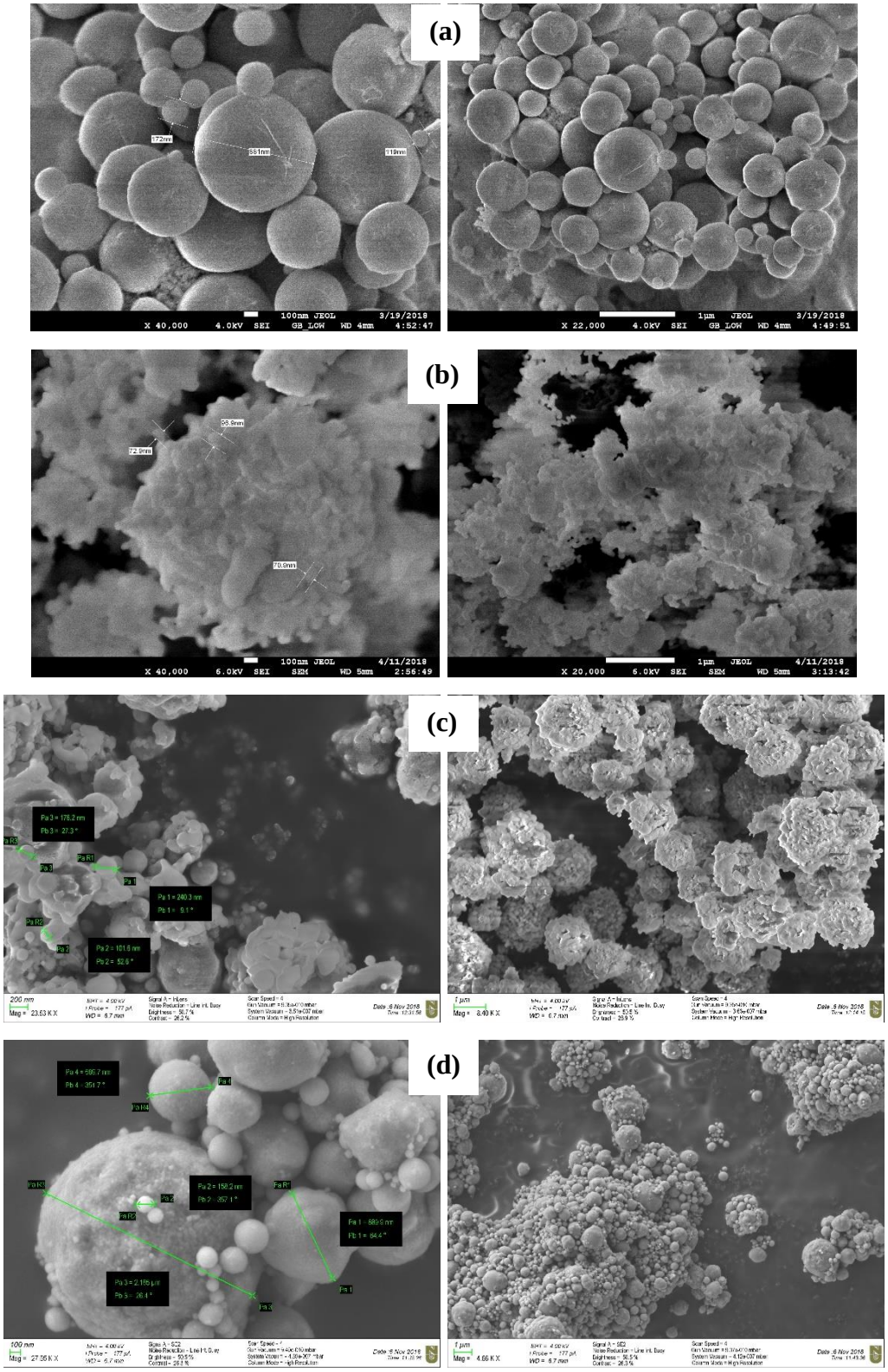


As it can be seen, originally LTO prepared by gas-state method has spherical shape particles and the particle size distribution is between 100 nm to 1 µm.

When it was prepared with Si nanopowder, the nanomixture of the spheres can be observed. As it is seen from Fig.3.3b, Si nanoparticles having much smaller volume are aggregated around larger LTO particles. So the whole nanomatrix is being consisted from the agglomerates sized up to 1 μm. The images of the powder prepared with addition of carbon sources are very different: the first one presents the sharp angled agglomerates similar to the ones in Fig. 3.3b, meanwhile the second one shows very smooth spherical shaped particles. For better understanding the morphology of the last two powders, TEM images were taken (see Fig.3.4).

***Figure 3.4: TEM images of: a)LTO/Si/Sucrose, b)LTO/Si/PEG.***

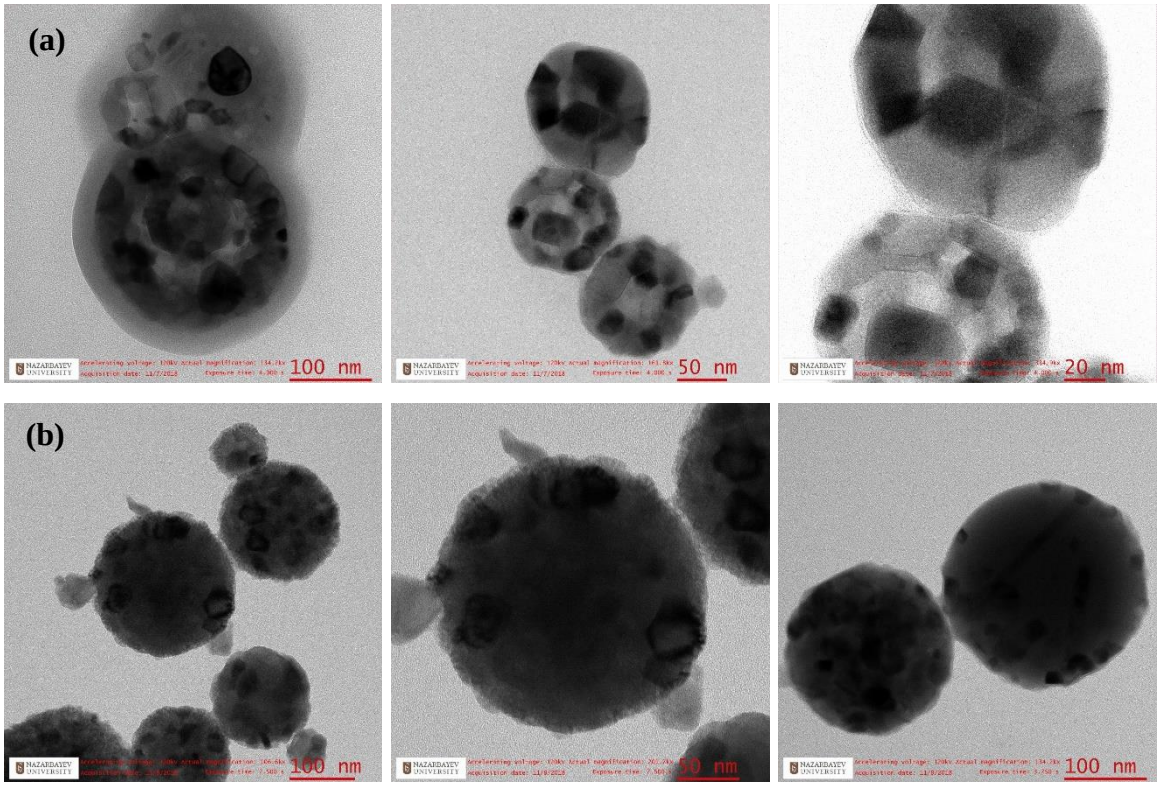


The structures illustrated in Fig.3.4 present spherical particles covered with amorphous layer, which is potentially carbon. As it can be seen, this layer covers

all particles and connects them to each other. Most probably, the dark spots in the spheres structure reveal the silicon particles. As it was assumed previously, LTO particles are covered with Si particles, which leads to the form of agglomerates in spherical shape. However, TEM images show that Si does not only covers LTO, but is also inserted into the structure of LTO, which enhances the electrochemical properties of the last one. Also, EDS analysis was performed and the results are shown below.

***Figure 3.5: EDS analysis of: a)LTO/Si/Sucrose, b)LTO/Si/PEG***

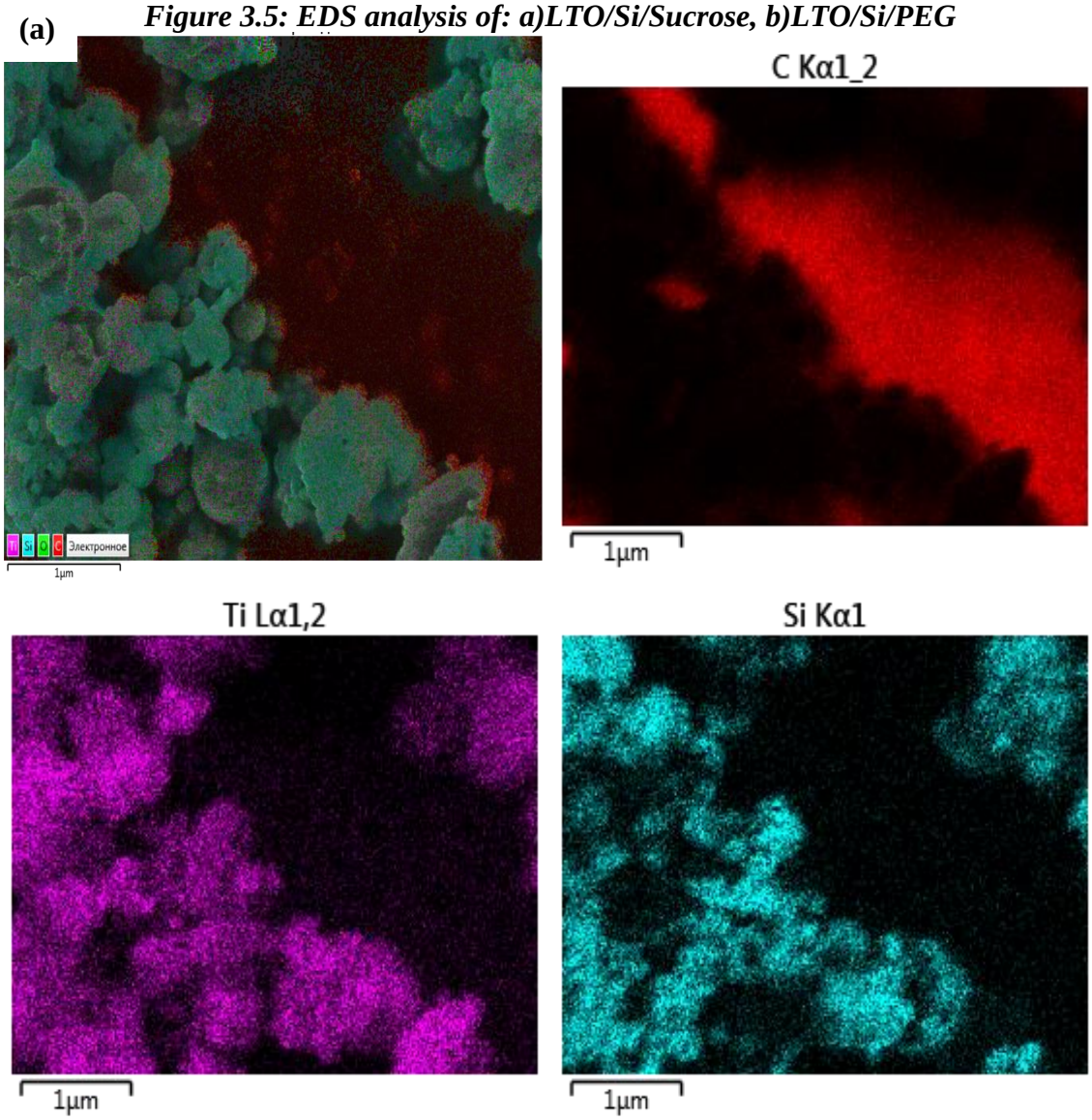

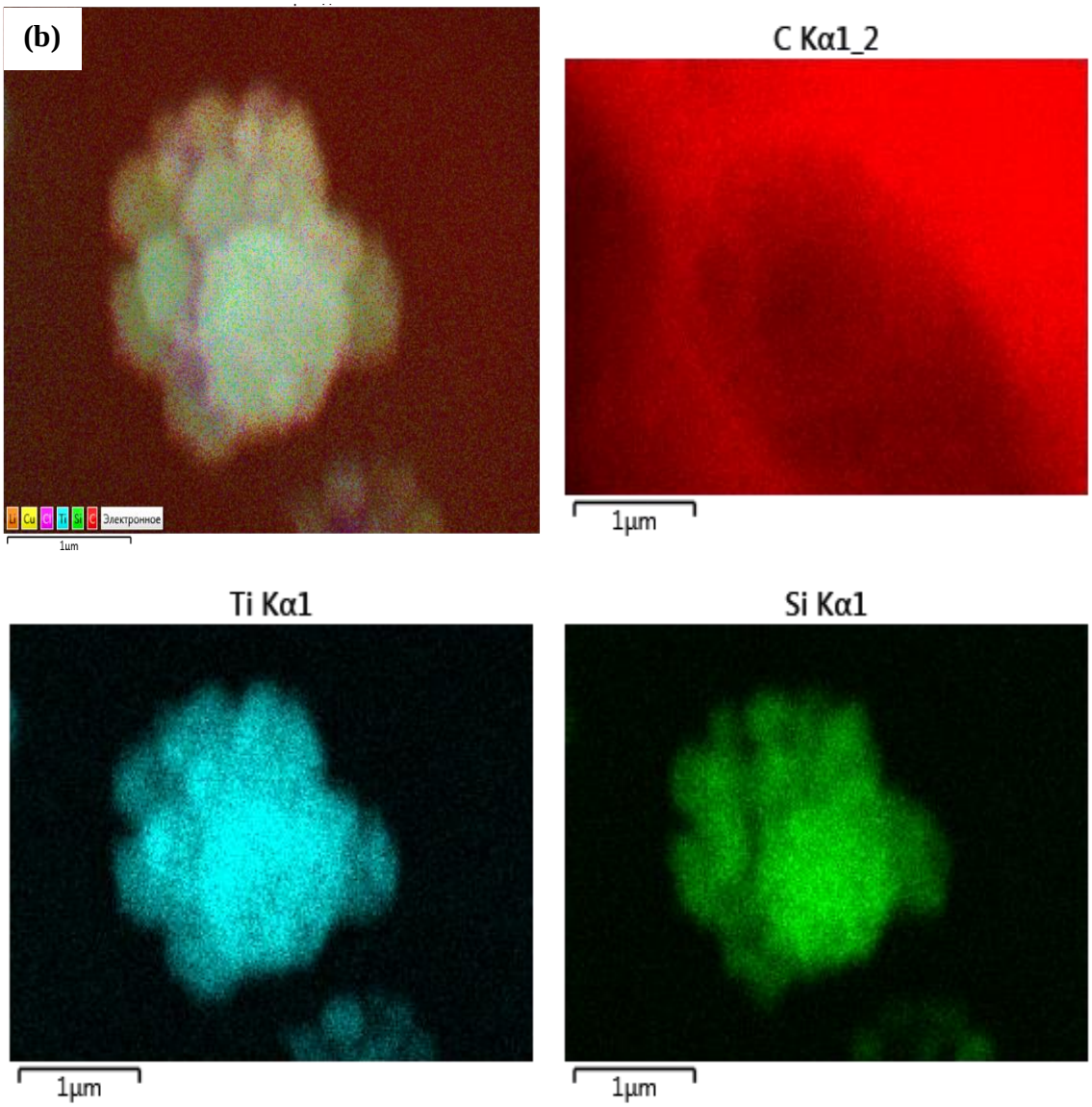


From EDS images in Fig. 3.5, a transcendent distribution of Si and Ti metals throughout the particles can be seen. It can be concluded, that the gas-state method such as spray-drying can provide very good mixing and coupling of the components within the material.

## 3.2 Results of electrochemical characterization

As it was described above, the battery testing was performed using Arbin battery tester in coin type half-cells. The results are presented on the graphs below.

***Figure 3.6: LTO/Si electrochemical results: a)Charge/Discharge profile; b)Cyclability***

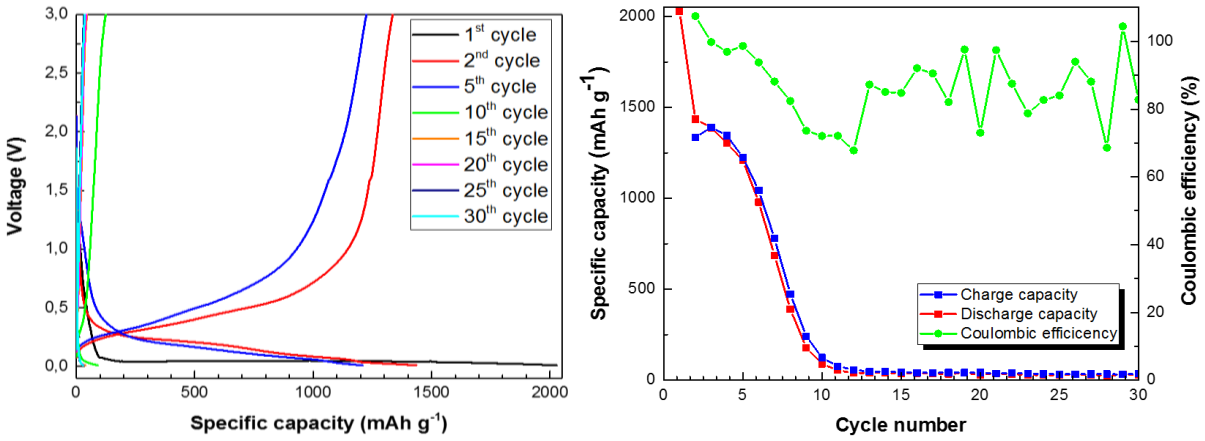


***Figure 3.7: LTO/Si/Sucrose electrochemical results: a)Charge/Discharge profile; b)Cyclability***

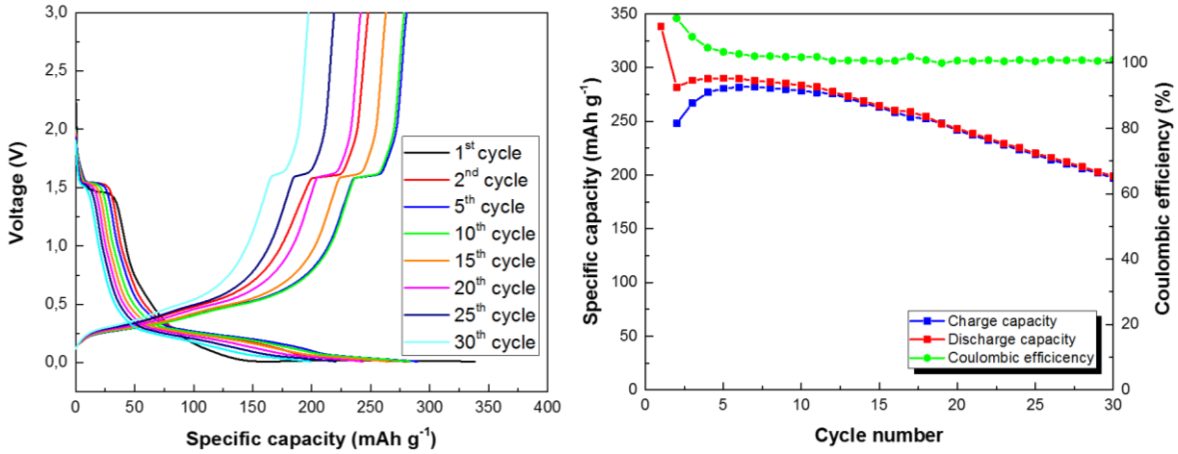

***Figure 3.8: LTO/Si/PEG electrochemical results: a)Charge/Discharge profile; b)Cyclability***

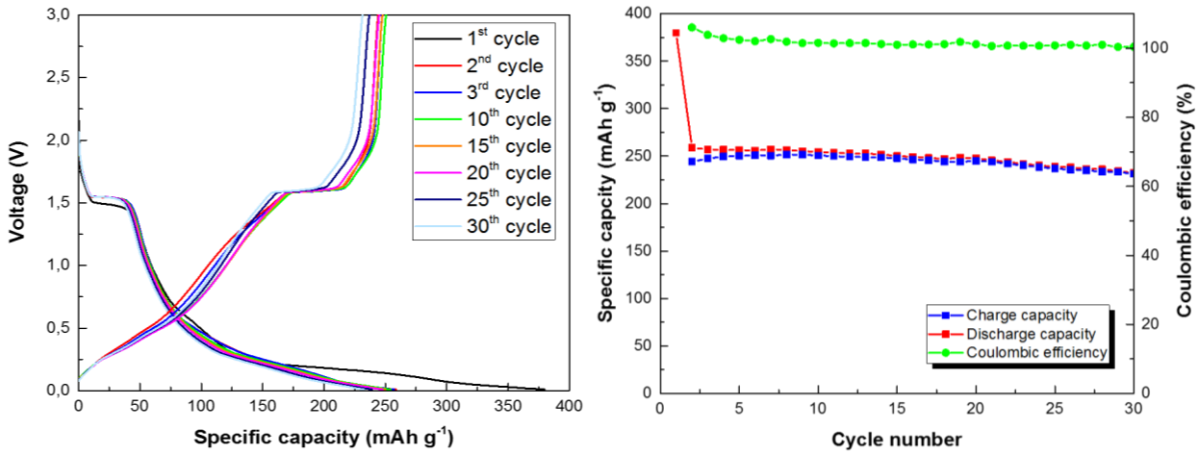


A plateau of the first discharge curve on all three graphs in Charge/Discharge profiles above corresponds to the transition of crystalline Si to amorphous phase. The region of smaller plateau at the point of 1.5 V, existing also on all three graphs, is referred to the intercalation of Li ions in the spinel structure of LTO [51]. Comparing the results of the first sample with two others, the significant improvements can be observed. Firstly, the stability of the material was remarkably enhanced. Both carbon containing samples show better performance in terms of capacity and cyclability. Despite the fact, that the first three cycles exhibit lower capacity than the sample of LTO/Si, the situation with further cycles is opposite. If LTO/Si sample presents almost zero capacity starting from $10^{th}$ cycle, the other two samples hold the capacity between 200 and 300 mAh $g^{-1}$. Also, it can be seen that the efficiency of the first sample dramatically fluctuates till the $30^{th}$ cycle, meanwhile the efficiency of other two samples is

very stable and is held at 100%, which means low capacity fading and good electrode stability. The retention of about 59 and 62% from its initial capacity was shown by LTO/Si/Sucrose and LTO/Si/PEG, respectively, after 30 cycles at 0.2 C; the capacity retention of LTO/Si was only 1.2%. The carbon containing samples were very similar to each other, though LTO/Si/PEG presented slightly better results in terms of capacity and efficiency.

Overall, it can be stated that electrochemical properties of LTO were successfully improved by Si nanopowder and presence of carbon source, even though the amount of the last one was small. As it was shown by TEM method the Si nanoparticles were inserted into the structure of LTO which prevents Si from fracturing due to the volume changes upon cycling and enhances the LTO capacity. It can be seen from the battery testing results, that the properties of the batteries were significantly improved.

### 3.3 Future work

Different synthesis temperatures can be studied to determine the most suitable one. The synthesis at 800 ºC was chosen based on the literature review, however, the XRD analysis showed that LTO was formed even at the inlet of the reactor, where the temperature was around 400-600 ºC. Therefore, from the engineering point of view, the synthesis temperature can be optimized further.

The same strategy can be applicable for flowrate of carrier gas. The effect of those parameters on the prepared powder can be studied.

Also, the proportions of precursor solution can be varied in order to investigate possibilities of controlling the materials morphology and structure. Along with this, the effect of carbon additive can also be studied.

The next step, which can be done in the project, is to modify the compressed nebulizer so that there was no air intake. Possibly, it can be located in the glove box with high-purity argon or nitrogen atmosphere, with insignificant air content. This can provide different content of the material, because the carbon will not be converted into carbon oxides.

# Chapter 4 – Conclusion

The LTO/Si, LTO/Si/Sucrose and LTO/Si/PEG were successfully synthetized by a gas-state method, mainly spray-drying, at one-step operation. XRD and EDS showed the presence of LTO and Si; CHNS showed the presence of carbon. According to SEM and TEM images, Si particles not only cover the LTO spheres, but are also inserted in the structure, which ensures enhanced electrochemical performance. TEM images showed the amorphous layer covering the particles of the carbon-containing samples, which was concluded to be carbon. The LTO/Si/Sucrose and LTO/Si/PEG presented the ameliorated performance in Li half-cells. Despite the fact that the samples showed lower discharge capacity in their 1$^{st}$ cycles, they exhibited more stable performance in terms of capacity and efficiency throughout the whole cycle life, showing the retention of about 59 and 62% from their initial capacity after 30 cycles at 0.2 C. The LTO/Si sample retained only 1.2% of its initial capacity. Therefore, it can be stated that the properties of the material were significantly improved using the additives. It can be stated that there was almost no difference between the powders prepared using different carbon sources, probably because of low carbon content resulted.

# References


[1] Manthiram A. Materials challenges and opportunities of lithium ion batteries. J Phys Chem Lett 2011; 2(3):176-184.

[2] Yanga L, Ravdelb B, Lucht BL. Electrolyte reactions with the surface of high voltage LiNi0.5Mn1.5O4 cathodes for lithium-ion batteries. ESL 2010; 13(8): A95-A97.

[3] Marom R, Amalraj SF, Leifer N, Jacob D, Aurbach D. A review of advanced and practical lithium battery materials. J Mater Chem 2011; 21:9938-9954.

[4] Orsini F, du Pasquier A, Beaudouin B, Tarascon JM, Trentin M, Langenhuizen N, de Beer E, Notten P. In situ SEM study of the interfaces in plastic lithium cells. J Power Sources 1998; 76(1):19-29.

[5] Landi BJ, Ganter MJ, Cress CD, DiLeo RA, Raffaelle RP. Carbon nanotubes for lithium ion batteries. Energy Environ Sci 2009; 2:638-654.

[6] Hou J, Shao Y, Ellis MW, Moore RB, Yi B. Graphene-based electrochemical energy conversion and storage: fuel cells, supercapacitors and lithium ion batteries. Phys Chem Chem Phys 2011; 13(34):15384-15402.

[7] Ge M, Rong J, Fang X, Zhou C. Porous Doped Silicon Nanowires for Lithium Ion Battery Anode with Long Cycle Life. Nano Lett 2012; 12(5):2318-2323.

[8] Wang Y, Wei H, Lu Y, Wujcik EK, Guo Z. Multifunctional Carbon Nanostructures for Advanced Energy Storage Applications. Nanomaterials 2015; 5(2):755-777

[9] Yang K, Lan H, Li P, Yu H, Qian S, Yan L, Long N, Shui M, Shu J. Strontium nitrate as a stable and potential anode material for lithium ion batteries. Ceram Int 2017; 43(13):10515–10520

[10] Bruce PG, Scrosati B, Tarascon JM. Nanomaterials for rechargeable lithium batteries. Angew Chem Int Ed 2008; 47(16):2930-2946.

[11] Wang Z, Zhou L, Lou XW. Metal oxide hollow nanostructures for lithium-ion batteries. Adv Mater 2012; 24(14):1903-1911.

[12] Li X, Wang C. Engineering nanostructured anodes via electrostatic spray deposition for high performance lithium ion battery application. J Mater Chem A 2013; 1:165-182.

[13] Bernholc J, Brenner D, Buogiorno Nardelli M, Meunier V, Roland C. Mechanical and electrical properties of nanotubes. Annu Rev Mater Res 2002; 32:347-375.

[14] DiLeo RA, Castiglia A, Ganter MJ, Rogers RE, Cress CD, Raffaelle RP, BJ Landi. Enhanced capacity and rate capability of carbon nanotube based anodes with titanium contacts for lithium ion batteries. ACS Nano 2010; 4(10):6121-6131.

[15] Wang B, Li X, Zhang X, Luo B, Jin M, Liang M, Dayeh SA, Picraux ST, Zhi L. Adaptable silicon–carbon nanocables sandwiched between reduced graphene oxide sheets as lithium ion battery anodes. ACS Nano 2013; 7(2):1437-1445.

[16] Wagemaker M, Mulder FM. Properties and promises of nanosized insertion materials for Li-ion batteries. Acc Chem Res 2013; 46(5):1206-1215.

[17] Li P, Qian SS, Yu HX, Yan L, Lin XT, Yang K, Long NB, Shui M, Shu J. $PbLi_2Ti_6O_{14}$: a novel high-rate long-life anode material for rechargeable lithium ion batteries. J Power Sources 2016; 330:45–54.

[18] Moretti A, Kim GT, Bresser D, Renger K, Paillard E, Marassi R, Winter M, Passerini S. Investigation of different binding agents for nanocrystalline anatase TiO2 anodes and its application in a novel, green lithium-ion battery. J Power Sources 2013; 221:419-426.

[19] Martha SK, Haik O, Borgel V, Zinigrad E, Exnar I, Drezen T, Miners JH, Aurbach D. $Li_4Ti_5O_{12}$/$LiMnPO_4$ Lithium-ion battery systems for load leveling application. J Electrochem Soc 2011; 158(7):A790-A797.

[20] Zhu GN, Chen L, Wang YG, Wang CX, Che RC, Xia YY. Binary $Li_4Ti_5O_{12}$- $Li_2Ti_3O_7$ nanocomposite as an anode material for Li-ion batteries. Adv Func Mater 2013; 23(5):640-647.

[21] Prakash AS, Manikandan P, Ramesha K, Sathiya M, Tarascon JM, Shukla AK. Solution-combustion synthesized nanocrystalline $Li_4Ti_5O_{12}$ as high-rate performance Li-ion battery anode. Chem Mater 2010; 22(9):2857-2863.

[22] Reddy ALM, Gowda SR, Shaijumon MM, Ajayan, PM. Hybrid nanostructures for energy storage applications. Adv Mater 2012; 24(37):5045-5064

[23] Kasavajjula U, Wang C, Appleby AJ. Nano- and bulk-silicon-based insertion anodes for lithium-ion secondary cells. J Power Sources 2007; 163:1003-1039.

[24] Zuoa X, Zhua J, Müller-Buschbaumb P, Cheng YJ. Silicon based lithium-ion battery anodes: A chronicle perspective review. Nano Energy 2017; 31:113–143

[25] Rahman M, Song G, Bhatt AI, Wong YC, Wen C. Nanostructured silicon anodes for high-performance lithium-ion batteries. Adv Funct Mater 2016; 26(5):647-678.

[26] Ryu J, Hong D, Choi S, Park S. Synthesis of ultrathin si nanosheets from natural clays for lithium-ion battery anodes. ACS Nano 2016; 10(2):2843–2851

[27] Chan CK, Peng H, Liu G, McIlwrath K, Zhang XF, Huggins RA, Cui Y. High-performance lithium battery anodes using silicon nanowires. Nat Nanotech 2008; 3:31–35.

[28] Chan CK, Patel RN, O'Connell MJ, Korgel BA, Cui Y. Solution-grown silicon nanowires for lithium-ion battery anodes. ACS Nano 2010; 4(3):1443-1450.

[29] Song T, Xia J, Lee JH, Lee DH, Kwon MS, Choi JM, Wu J, Doo SK, Chang H, Park WI, Zang DS, Kim H, Huang Y, Hwang KC, Rogers JA and Paik U. Arrays of sealed silicon nanotubes as anodes for lithium ion batteries. Nano Lett 2010; 10(5):1710-1716.

[30] Liu XH, Huang S, Picraux ST, Li J, Zhu T, Huang JY. Reversible nanopore formation in Ge nanowires during lithiation–delithiation cycling: an in situ transmission electron microscopy study. Nano Lett 2011; 11(9):3991-3997.

[31] Yin X, Chen L, Li C, Hao Q, Liu S, Li Q, Zhang E, Wang T. Synthesis of mesoporous SnO2 spheres via self-assembly and superior lithium storage properties. Electrochim Acta 2011; 56(5):2358-2363.

[32] Ye J, Zhang H, Yang R, Li X, Qi L. Morphology-controlled synthesis of $SnO_2$ nanotubes by using 1D silica mesostructures as sacrificial templates and their applications in lithium-ion batteries. Small 2010; 6:296-306.

[33] Chen JS, Ng MF, Wu HB, Zhang L, Lou XW. Synthesis of phase-pure $SnO_2$ nanosheets with different organized structures and their lithium storage properties. Cryst Eng Comm 2012; 14:5133-5136.

[34] Su X, Wu Q, Li J, Xiao X, Lott A, Lu W, Sheldon BW, Wu J. Silicon-based nanomaterials for lithium-ion batteries: a review. Adv Energy Mater 2014; 4:1– 23

[35] Kim C, Norberg NS, Alexander CT, Kostecki R. Mechanism of phase propagation during lithiation in carbon-free $Li_4Ti_5O_{12}$ battery electrodes. Adv Funct Mater 2013; 23:1214–1222

[36] Chen C, Agrawal R, Wang C. High performance $Li_4Ti_5O_{12}$/Si composite anodes for Li-ion batteries. Nanomaterials 2015; 5(3):1469-1480.

[37] Stenina IA, Kulova TL, Skundin AM, Yaroslavtsev AB. Carbon composites as anode materials for lithium-ion batteries. Rev Adv Mater Sci 2017; 49:140-149

[38] Hong JE, Oh RG, Ryu KS. $Li_4Ti_5O_{12}/Co_3O_4$ composite for improved performance in lithium-ion batteries. J Electrochem Soc 2015; 162(10):A1978-A1983

[39] Prakash S, Manikandan P, Ramesha K, Sathiya M, Tarascon JM, Shukla AK. Solution-combustion synthesized nanocrystalline $Li_4Ti_5O_{12}$ as high-rate performance Li-ion battery anode. Chem Mater 2010; 22:2857–2863

[40] Jiang C, Hosono E, Ichihara M, Honma I, Zhoua H. Synthesis of nanocrystalline $Li_4Ti_5O_{12}$ by chemical lithiation of anatase nanocrystals and postannealing. J Electrochem Soc 2008; 155(8):A553-A556

[41] Huang J, Jiang Z. The synthesis of hollow spherical $Li_4Ti_5O_{12}$ by macroemulsion method and its application in Li-ion batteries. ESL 2008; 11(7):A116-A118

[42] Cheng L, Li X, Liu H, Xiong H, Zhang P, Xia Y. Carbon-coated $Li_4Ti_5O_{12}$ as a high rate electrode material for Li-ion intercalation. J Electrochem Soc 2007; 154(7):A692-A697

[43] Kavan L, Gratzel M. Facile synthesis of nanocrystalline $Li_4Ti_5O_{12}$ spinel. exhibiting fast Li insertion. ESL 2002; 5(2):A39-A42 2002

[44] Jin Y, Min K, Shim H, Seo S, Hwang I, Park K, Kim D. Facile synthesis of nano-$Li_4Ti_5O_{12}$ for high-rate Li-ion battery anodes. Nanoscale Res Lett 2012; 7(10)

[45] Birrozzi A, Copley M, von Zamory J, Pasqualini M, Calcaterra S, Nobili F, Di Cicco A, Rajantie H, Briceno M, Bilbe E, Cabo-Fernandez L, Hardwick LJ, Bresser D, and Passerinia S. Scaling up "Nano" $Li_4Ti_5O_{12}$ for high-power lithium-ion anodes using large scale flame spray pyrolysis. J Electrochem Soc 2015; 162(12):A2331-A2338

[46] Kim JH, Kang YC. Electrochemical Properties of Nano-sized $Li_4Ti_5O_{12}$ Powders Prepared by Flame Spray Pyrolysis. Int J Electrochem Sci 2013; 8:3379 - 3389

[47] Wu F, Wang Z, Li X, Guo H, Yue P, Xiong X, He Z, Zhang Q. Characterization of spherical-shaped $Li_4Ti_5O_{12}$ prepared by spray drying. Electrochim Acta 2012; 78:331–339

[48] Ju SH, Kang YC. Effects of preparation conditions on the electrochemical and morphological characteristics of $Li_4Ti_5O_{12}$ powders prepared by spray pyrolysis. J Power Sources 2009; 189:185–190

[49] Chevriera VL, Liu L, Ba Le D, Lund J, Molla B, Reimer K, Krause LJ, Jensen LD, Figgemeier E, Ebermana KW. Evaluating Si-Based Materials for Li-Ion Batteries in Commercially Relevant Negative Electrodes. J Electrochem Soc 2014; 161:A783–A791

[50] Barron M, Young TJ, Johnston KP, Williams R. Investigation of processing parameters of spray freezing into liquid to prepare polyethylene glycol polymeric particles for drug delivery. AAPS Pharm Sci Tech 2003; 4(2):E12

[51] Sanbayeva A, Molkenova A, Sultanov M, Karymsakov A, Myung ST, Bakenov Z. $Li_4Ti_5O_{12}$/Si/c-PAN Composite as an Anode Material for Lithium-Ion Batteries. Manuscript.